Response to Noemi Petra (Referee)

The paper applies an adjoin-based inversion method to an inverse problem governed by a one-dimensional transport equation. The inversion is for the accumulation, melting and the initial distribution of age depth parameters from ice age measurements. The inverse problem is formulated as a nonlinear least-squares optimization problem whose cost functional is the misfit between ice age observations and model predictions. Tikhonov regularization is added to the cost functional to render the problem well-posed and account for observational error. The authors show that the reconstructions of the accumulation parameter field deteriorates when the noise added to synthetic observations increases, and the quality of the reconstruction depends on the available observations. The method is also applied with real observations extracted from the James Ross Island's ice cores. I find the topic of the paper interesting. To the best of my knowledge, this paper is the first to report on an adjoint-based solution method applied to inverse problems using vertical ice information. However, I would like to point out that the inversion method itself is not novel, as claimed in the abstract and conclusions.

We agree with the reviewer that the numerical method itself is not novel, as it is an inverse problem governed by the advection equation, but we are solving the inversion of paleo-accumulation records in a new way. To clarify this point we have rewritten the abstract and changed "novel adjoint method" to "novel approach to reconstruct an ice core".

Below I list my detailed comments:

1. Title and Abstract:

(a) I sugest replacing "adjoin method" with "adjoint-based method" (the method is not adjoint, it is based on adjoint to compute gradient information).

Done.

(b) It is not easy to understand from the abstract what exactly is the inverse problem, what are the inversion parameters, and what are the observations.

We have rewritten the second line of the abstract as "We present approach to reconstruct a climatic record by both optimally dating an ice-core from sparse observations and deriving from it a detailed accumulation history."

(c) It is not clear what the authors mean by "gaps in the data".

We have written "gaps in the age-depth observations"

2. Sections: Section 1.

Again, we are not claiming anything new in the numerical model, as we are following techniques described in Petra and Stadler (2011), but we are showing how it can be used to incorporate vertical velocity measurements to improve the ice-core chronology and the retrieval of paleo-accumulation. We have rewritten P3 L16-L23 to make this point clearer.

We have written a more generic "ice-flow properties" as different authors use different parameters to represent ice-flow properties.

There is none, well spotted. That was a typo result of a rewriting of the manuscript.

Done

Done.

We have rewritten the paragraph and introduce a new equation to make clear where the age equation comes from.

Yes, that would be the normal case. We have added the discrete operator Pd, which is described in Eq. 4.

Done.

We believe that now that we have made that clear in equation (1) that information would be repetitive.

(f) The language after equation (4) talking about the "formal Lagrange approach" is a bit vague (especially for the cryosphere community).

We believe that the first sentence is more general that vague but, in any case, we describe the method in the second sentence and in equation (5).

(g)After eq. (5), I recommend explaining that the gradient of the cost J can be found by requiring that variations of the Lagrangian with respect to the forward and adjoint variables vanish.

Done. We have rewritten the paragraph and introduced and appendix where we verify this property.

(h) I recommend adding the details for the derivation of the adjoint into an appendix section. I am surprised to see the positive sign for @ t and w under the partial derivative. Was the gradient checked via finite diferences? It would be great to show this verification in the numeric section.

Done. We have included an appendix. In the synthetic case we have the analytical solution and an analytical expression for J, so everything has been checked.

(i) Eq. (6): the boundary condition should hold for all t [0;T], and the final condition should hold for all z [0;H].

We have rewritten the boundary conditions so that they are clearer.

(j) I recommend calling the "control equations" gradients and not setting these to zero, since this is true (close to zero) only at the (optimal) solution. (This will also avoid the need to repeat equations in (9).)

Done

Same comment as for the adjoint, please add the derivation of the gradient in the appendix.

Done.

(k) I suggest splitting Section 2.2 into two sections, namely 2.2. inverse model/problem section and 2.3. the solution method which would show the adjoin-based approach, including everything from section 2.3. (The title of Sec. 2.3. is misleading, it suggests that this section covers the numerical solution/results.)

We don't fully understand the point but reading comment (m) we suspect that the reviewer hasn't realized that we describe the numerical solution techniques for the PDEs at the end of the Section. As they are included, the Section title is certainly not misleading.

(l) Why is x either of the three parameters? Is the inverse problem solved for one inversion parameter at a time?

Not necessarily, we are shortening the notation.

(m) I may have missed it, how are the forward and adjoint problems solved?

The numerical technique to solve forward and adjoin problems is described in Section 2.3. We use an operator combined Semi-Lagrangian Crank-Nicholson scheme.

(n) Typical value for c in the context of the Armijo condition is 10

Is that personal experience or there is a reference with typical values for c? We will be happy to add that information. Armijo used 0.5 in his original paper and is meant to work with any value between $0<c<1$.

(o) It would be useful for the readers to see the L-curve plot.

We believe that would be too technical for the paper and it wouldn't add more information to the accumulation inversion method.

Section 3.

(a) How much noise was added to the data? (line 5)

I am afraid we cannot write all the information about the section in one introductory sentence. The reader will find that we add different errors to different runs, as one of the aims of the paper is looking at the effect of noise on the data, and all that information is described a few paragraphs down.

(b) It is not clear (from the text) which colors (lines) show the reference accumulation and age depth.

All that information is in the figure caption.

(c) Eq. 13 zk versus zk. I also recommend showing the dependence of on z, by defining (z).

Done.

(d) The steepest descent is known to perform poorly compared to not only Hessian-based methods but also compared to more sophisticated gradient-based methods (e.g., nonlinear CG). I am very surprised to see the very small number of iterations (for the steepest descent method).

Sorry about the typo, number of iterations is 100-200 and not 10-20. (That would have been amazing.) In any case, the reason we haven't used a more sophisticated method is because one iteration takes about a second to be solved in a normal desktop and we have never felt the need of increase the efficiency of the computations. We are considering now more complicated ice-flow models and we are looking at more effective methods.

Numerical details have been replaced by stopping criteria. We have tried several of them variation of accumulation per iteration, difference with the reference solution, reduction of J absolute or relative to the previous solution or to the first solution. All of them give similar results and we believe it doesn't add anything to the paper including all those numerical details.

The objective of Figure 1 is supporting the Section 3.1 and not the other way around. The figure is described in the third to last paragraph of Section 3.1. Recovered and reference age-depth are nearly identical, as explained in the text, there is nothing that can be done visually to differentiate them, this is one of the conclusions of the paper: with a rough estimate of the accumulation the recovered age-depth is surprisingly close to the reference solution (Similar to Fudge, 2014).

We have replaced "measure the sensitivity" by "study the sensitivity" to make it clearer. However, we believe that "parameter uncertainty" it has a very clear meaning.

For the given forward model, it does make sense to present the inversion of the three parameters: the simplest 1D ice velocity, assuming we know the shape function, is going to depend on accumulation and melting, and as we are interested in transient age-depth, the initial age-depth is going to be unknown. Using them or not depends of the properties of the dome where the ice core has been extracted. In the case of James Ross Island, melting is negligible as the dome is very shallow and the modelling time is so sort that we can simulate the age-depth for a longer time so that the initial age-depth is unimportant. That is not the case in all the ice-core sites and we believe that the utility of having the inversion described in the paper outweighs the complication introduced by it. We

have rewritten Section 3.2 so that why don't we use melting or initial age distribution is clearer.

Sections 4 and 5 may have some terminology inconsistency that, thanks to the reviewer comments bellow, we have corrected but we don't think that the language is causal and if the reviewer is referring to P12 line26 line in the old manuscript, we cannot find any "grammar issue" but we have rewritten the sentence to make it clearer.

Conclusions have one paragraph of motivation, one on methodology, one summarizing the results and another one with further work. It is impossible to avoid some repetition between conclusions and the rest of the paper. We believe is good practice to finish the paper with a small summary.

We believe is not an strong claim but the most general comment possible. It is like saying that a bad omelette is a consequence of bad ingredients or bad cooking.

We have replaced "model inversion" by "inverse problem" that is more commonly used, but we think that "information recovered" has a clear meaning.

We use a basic Monte Carlo method. It is described in the previous Section (Sec. 3), second to last and last paragraphs.

We don't understand the reviewer comment. We use word gap to refer to an unfilled space or interval. By perfectly sampled, we mean that we have taken all the possible samples from the age-depth. (We can only do that with the synthetic data in Section 3.1.). And by retrieved profile we mean the profile that we have recovered.

We have rewritten the sentence to differentiate between age-depth observations and the resulting Chronology or improved and continuous age-depth.

We would associate "noise level" with the data but the "uncertainty" in line 21 is referring to the lack of certainty introduced in the paleo-accumulations due to the "uncertainty" or "noise level" in the ice-core chronology.

We don't understand the comment, we think that the term constrained optimization is well spread in different areas of control theory, and using the Lagrange multipliers one of the most common techniques.

Inferring paleo-accumulation records from ice-core data by an adjoint-based method: Application to James Ross Island's ice core

Carlos Martín[1]**, Robert Mulvaney**[1]**, G. Hilmar Gudmundsson**[1]**, and Hugh Corr**[1]

[1]British Antarctic Survey, UK

Correspondence to: Carlos Martín (cama@bas.ac.uk)

Abstract

Ice cores contain a record of snow precipitation that includes information about past atmospheric circulation and mass imbalance in the polar regions. We present a novel approach to reconstruct a climatic record, by both optimally dating an ice-core and deriving from it a detailed accumulation history, that uses an adjoint-based method. The motivation of our work is the recent application of phase sensitive radar which measures the vertical velocity of an ice column. The velocity is dependent on the history of subsequent snow accumulation, compaction and compression; and in our inverse formulation of this problem, measured vertical velocity profiles can be utilized directly thereby reducing the uncertainty introduced by ice flow modelling. We first apply our method to synthetic data in order to study its capability and the effect of noise and gaps in the age-depth observations. The method is then applied to the ice core retrieved from James Ross Island, Antarctica. We show that the method is robust and that the results depend on quality of the age-depth observations and the derived flow regime around the core site. The method facilitates the incorporation of increasing detail provided by ice-core analysis together with observed full-depth velocity in order to construct a complete climatic record of the polar regions.

1 Introduction

A layer of snow deposited at some position and time on the surface of an ice sheet has today a burial rate and depth that is dependent on the weight and amount of snow accumulated above it, its metamorphosis to ice and the flow of the ice sheet. When the ice core is extracted, the chemical constituents trapped in the ice contain information of the climatic conditions during the time of deposition.

Dating the ice-core is paramount in order to interpret the climatic record. Different methods are used to establish the ice-core timeline, mainly: annual layer counting, localization of dated volcanic eruptions in the record, comparison of chemical species with other ice-cores, and ice flow modelling. Commonly, the ice-core chronology is obtained by a combination of methods

(e.g., Hammer et al., 1978; Parrenin et al., 2007a; Lemieux-Dudon et al., 2010). Annual layer counting and the localization of known volcanic events offer accurate dating, but their use is restricted to the top of the ice-core or to sparse sections of the record.

Ice-core dating relies on ice-flow models in sections where direct chronological information is unavailable or incomplete. The assumption made is that the record of snow accumulation is related to past cloud temperatures that, in turn, are derived from ice core isotope analysis (e.g., Watanabe et al., 2003; Parrenin et al., 2007b). However, this assumption can not be used on coastal areas of Antarctica or Greenland (Bromwich and Robasky, 1993; Kapsner et al., 1995) where the main driver of change in accumulation is atmospheric circulation and not the thermodynamic equilibrium of the atmosphere. However, recent advances in ice core data analysis provide detailed chronologies for ice cores located in coastal areas using layer counting (e.g., Rasmussen et al., 2006; van Ommen and Morgan, 2010) or transferring timelines from reference ice-cores using stratigraphic links (e.g., Ruth et al., 2007; Lemieux-Dudon et al., 2010). The aim of this paper is to use a detailed chronology such as those, derived independently of temperature reconstructions, in order to obtain a record of paleo-accumulation.

Previous work has estimated paleo-accumulation and unknown ice-flow properties in order to extend the age-depth record beyond the confines of layer counting or stratigraphic links. Typically, an inverse method based on direct search is applied (e.g., Dansgaard and Johnsen, 1969) or, more recently, on Monte-Carlo techniques (e.g., Parrenin et al., 2001; EPICA community members, 2004; Parrenin et al., 2007b). Here, our approach is to apply an adjoint-based method for constrained optimization, commonly employed in computational fluid dynamics (CFD) for inverse problems that are governed by partial differential equations (e.g., Petra and Stadler, 2011).

The motivation of our work is the increasing interest in climatic records extracted from high-resolution ice cores located in coastal areas of Antarctica and Greenland (e.g., van Ommen and Morgan, 2010; Mulvaney et al., 2012). We have taken advantage of the recent development of a phase sensitivity radar, that allow the direct measurement of the present vertical velocity full-depth along the ice-core (Corr et al., 2002; Jenkins et al., 2006), this greatly reduces the uncertainty introduced by ice-flow modelling (Kingslake et al., 2014). In addition, recent advances in multi-

3

ice-core multi-component analysis has improved the detail in ice core chronology (e.g., Rasmussen et a
2006; Ruth et al., 2007; Lemieux-Dudon et al., 2010).

We first describe the method in Section 2 and its application to synthetic and existing data
from James Ross Island ice core data (Mulvaney et al., 2012, 2014) in Section 3. At the time
of writing this manuscript we do not have a suitable location where both velocity derived from
phase sensitive radar and a detailed ice core timeline is avaliable. For simplicity, we have as-
sumed that the flow of ice follows a (Dansgaard and Johnsen, 1969) analytical approximation
for the synthetic data (Sec. 3.1) and a shallow ice approximation (e.g., Hutter, 1983) combined
with the measured compaction for the James Ross Island ice core case (Sec. 3.2).

2 Methodology

2.1 Description of the problem: Forward model.

The combined result of snow accumulation, compaction and compression is that a particle of ice
deposited in the surface of a summit of ice-thickness H is transported with a velocity (u, v, w)
within the ice. The age of a particle of ice A, represents the time elapsed for a particle of ice to
get transported from the surface to a given position (x, y, z), where z represents the vertical.

The age of a particle of ice can be expressed with the pure advection equation (e.g., Hindmarsh,
2001), because the increase in the age of a particle of ice is identical to the increase in time,

$$\frac{DA}{Dt} = 1,$$

where D represents the material derivative. In this paper, we consider that the distribution of
the age varies in time, from a given initial state A_0 to the present ($t = T$), but we neglect the
effect of horizontal advection and the local variation of thickness through time ($\frac{\partial H}{\partial t} = 0$). The

4

age of ice can then be expressed as,

$$\partial_t A + w \, \partial_z A = 1, \qquad 0 \le z \le H, \, 0 \le t \le T$$
$$A(z,0) = A_0, \qquad\qquad 0 \le z \le H,$$
$$A(H,t) = 0, \qquad\qquad 0 \le t \le T. \qquad (1)$$

We assume that the spatial variation of the velocity only depends on rheology and not on time dependent variables such as surface accumulation or ice thickness (e.g., Parrenin et al., 2007a). This assumption is supported by the perturbation analysis of Wilchinsky and Chugunov (1997) for isothermal ice. Considering the conservation of mass, the vertical velocity is

$$w(z,t) = -m(t) + [-a(t) + m(t)] \, \eta(z), \qquad (2)$$

where a is the surface accumulation rate, m the basal melt rate, and η is the shape function (sometimes referred to as thinning function). For the sake of simplicity, we refer to the surface accumulation rate and basal melt rate as accumulation and melting, as there is no possible ambiguity in this paper.

2.2 Inverse model

The inverse problem can be formulated as finding the records of accumulation $a(t)$ and melting $m(t)$, and the initial distribution of age-depth $A_0(z)$, that minimize the difference between

observations and model results:

$$\min_{a,m,A_0} J(a,m,A_0;A) := \frac{1}{2} \int\limits_0^H \frac{[A(z,T) - A_d]^2}{\sigma_d} P_d \, dz$$

$$+ \frac{\gamma_a^R}{2} \int\limits_0^T (\partial_t a)^2 dt + \frac{\gamma_m^R}{2} \int\limits_0^T (\partial_t m)^2 dt$$

$$+ \frac{\gamma_{A_0}^R}{2} \int\limits_0^H (\partial_z A_0)^2 dz, \tag{3}$$

where γ_a^R, γ_m^R and $\gamma_{A_0}^R$ denote the weight of the Tikhonov regularization for accumulation, melting and initial age-depth distribution. A_d is the measured age of ice, σ_d its estimated uncertainty and P_d is the point measurement operator for discrete data (Petra and Stadler, 2011),

$$P_d(z) = \sum_{j=1}^{N_d} \delta(z - z_j) \quad \text{for } j = 1, ..., N_d, \tag{4}$$

where N_d is the number of point measurements and $\delta(z - z_j)$ is the Dirac delta function. $a(t)$, $m(t)$ and $A_0(z)$ are functions of time or space that we want to find; A depends on them and it can be obtained by solving Equation 1. J is a functional that depends on $a(t)$, $m(t)$, $A_0(z)$ and $A(z,t)$.

We follow a Lagrange approach (e.g., Tröltzsch, 2010), that includes a Lagrangian multiplier function λ in order to find the solution of the minimization problem (Eq. 3) constrained by the

forward model (Eq. 1).

$$\mathcal{L}(a, m, A_0; A, \lambda) = J(a, m, A_0; A)$$

$$+ \int\limits_0^T \int\limits_0^H \lambda(\partial_t A + w\,\partial_z A - 1)\,dz\,dt$$

$$+ \int\limits_0^H \lambda(z,0)\,[A(z,0) - A_0]\,dz \qquad (5)$$

The optimal solution is obtained by setting the variations (functional derivatives) of the Lagrangian $\mathcal{L}$ with respect all variables to zero. The Lagrangian in Equation 5 verifies that setting the functional derivative of the Lagrangian with respect to the Lagrangian multiplier to zero ($\delta_\lambda \mathcal{L} = 0$) is equivalent to the forward problem, also known as state equation (Eq. 1). The details of the derivation of the optimal system of equations are described in the Appendix.

Setting the variations of $\mathcal{L}$ with respect to the age ($\delta_A \mathcal{L} = 0$) leads to the adjoint problem for λ, that in the strong form can be written as,

$$\partial_t \lambda + \partial_z(w\,\lambda) = 0, \qquad 0 \le z \le H,\, 0 \le t \le T$$

$$\lambda(z,T) = \frac{A_d - A}{\sigma_d} P_d, \qquad 0 \le z \le H,$$

$$\lambda(0,t) = 0, \qquad 0 \le t \le T. \qquad (6)$$

Finally, the so-called control equations, are obtained by calculating the variations of $\mathcal{L}$ with respect to accumulation, melting and initial distributions of age and setting them to zero ($g_a =$

$\delta_a \mathcal{L} = 0$, $g_m = \delta_m \mathcal{L} = 0$ and $g_A = \delta_{A_0} \mathcal{L} = 0$):

$$g_a = -\int_0^H \eta\,(\lambda\,\partial_z A)\,dz - \gamma_a^R \partial_t^2 a = 0,$$

$$g_m = \int_0^H (\eta - 1)(\lambda\,\partial_z A)\,dz - \gamma_m^R \partial_t^2 m = 0,$$

$$g_A = -\lambda(z,0) - \gamma_A^R \partial_z^2 A_0 = 0. \tag{7}$$

2.3 Numerical Solution

The system of Equations composed by the state equation (Eq. 1), the adjoint equation (Eq. 6) and the gradients (Eq. 7) represent a complex non-linear system of equations. In order to solve the system, we use a steepest decent method (e.g., Petra and Stadler, 2011).

First we assume initial solutions for accumulation, melting and initial distribution of age (a^k, m^k and A_0^k). We then solve the state equation (Eq. 1), and using the inferred solution of age A^k, we solve the adjoint equation backward in time to obtain the solution of the Lagrange multiplier λ^k.

In order to update the solution for accumulation, melting and initial distributions of age and temperature, we increase them in the direction of steepest descent of the Lagrangian.

$$
\begin{aligned}
a^{k+1} &= a^k + \beta_a g_a, \\
m^{k+1} &= m^k + \beta_m g_m, \\
A_0^{k+1} &= A_0^k + \beta_A g_A,
\end{aligned}
\tag{8}
$$

where β_a, β_m are β_A are parameters.

The values of β_a, β_m and β_A are calculated each iteration using a backtracking line search algorithm (e.g., Dennis and Schnabel, 1996, §6.3.2). The method assumes sufficiently large ini-

tial values for β_a, β_m and β_A, that are successively halved until the corresponding decrease in the objective function J (Eq. 3) fulfil the Armijo (1966) condition,

$$J(x^k) - J(x^{k+1}) \geq -c\,\beta_x\,g_x^2 \,, \tag{9}$$

where x represents the state variables a, m or A_0; g_x the respective gradients of the objective
function g_a, g_m or g_A; β_x the parameters β_a, β_m or β_A; and the constant c is fixed to $c = 10^{-2}$.

The values of γ_a^R, γ_m^R and $\gamma_{A_0}^R$, are chosen by inspection of the L-curve (e.g., Hansen, 2000). The L-curve is a plot of the norm of the regularization term ($\int_0^T (\partial_t a)^2 dt, \int_0^T (\partial_t m)^2 dt$ or $\int_0^H (\partial_z A_0)^2 dz$) versus the difference in age-depth between observation and model results ($\int_0^H P_d [A(z,T) - A_d]^2 / \sigma_d\, dz$) for different values of the regularization parameter. The L-
curve has two distinctive sections: for sufficiently small values of the regularization param-eter, the differences between data and model dominate the objective function, and a gradual increase in the smoothing of the solution implies a gradual increase in the differences between data and model; conversely, for sufficiently large values of the regularization parameter, the regularization term dominates the objective function, and a gradual increase in the smoothing
of the solution translates into sharper differences between data and model. The curve typically is L-shaped, and hence its name. The regularization parameters are chosen so that their corre-sponding terms in the objective function sit on the L-curve between these two sections, that is, the corner of the L.

Regarding the numerical techniques, we solve the state equation (Eq. 1) and the adjoint
equation (Eq. 6), by using a operator combined Semi-Lagrangian Crank-Nicholson algorithm (SLCN) (Spiegelman and Katz, 2006) in a equispaced grid of elevation $\{z_i\}$.

The second order two-level Semi-Lagrangian scheme (e.g., Staniforth and Côté, 1991) solves the advection terms as an ordinary differential equation along the trajectory that connects from some take-off elevation z_* at time $t = (n)\Delta t$ to a regular grid point z_i at time $t = (n+1)\Delta t$ in
the state equation, that is solved forward in time, and at time $t = (n-1)\Delta t$ in the adjoint equa-tion, that is solved backward in time ($\Delta t \to -\Delta t$, $w \to -w$). The Crank-Nicolson algorithm is used to discretize the diffusive terms with a central difference.

9

The discretized state equation (Eq. 1) and the adjoint equation (Eq. 6), using the SLCN method are respectively,

$$A_i^{n+1} = 1 + A_*, \tag{10}$$

$$(1 - \frac{\Delta t}{2}\delta w_i)\lambda_i^{n-1} = (1 + \frac{\Delta t}{2}\delta w_i)\lambda_*; \tag{11}$$

5 where δ denotes the gradient discrete operator

$$(\nabla f)|_{z_i} \approx \delta f_i = \frac{f_{i+1} - f_{i-1}}{2\Delta z},$$

and $()_*$ denotes the value at the take-off position z_* and time $t = (n)\Delta t$.

3 Results

3.1 Recovering accumulation from synthetic age-depth observations

10 In order to study the capability of our method to recover paleo-accumulation from age-depth observations,we have generated synthetic observations by adding random noise to a reference solution.

The reference accumulation solution varies over 10 kyr as,

$$a(t) = [0.2 + 0.1\sin(2\pi t/\tau_1) + 0.05\sin(2\pi t/\tau_2)] \text{ m yr}^{-1},$$

15 where $\tau_1 = 10$ kyr, and $\tau_2 = 1$ kyr. Figure 1 shows the reference accumulation and age-depth.

In this Section, we assume that there is no melting, and that the shape function (Eq. 2) follows Dansgaard and Johnsen (1969),

$$\eta(z) = \begin{cases} \frac{z - z_k/2}{H - z_k/2} & z_k \leq z \leq H \\ \frac{z^2/2}{z_k(H - z_k/2)} & 0 \leq z \leq z_k \end{cases}, \tag{12}$$

10

where z_k is a parameter that we fix to $z_k = 0.3\,H$. In addition, we assume that the initial age distribution ($A(t = 0)$) is exact and that it is a steady-state solution of the velocity distribution at time $t = 0$.

We first check our model by applying it to the age-depth derived from the reference accumu-
lation. The algorithm (Sec. 2.3) converges in 100-200 iterations, depending on the initial guess and the stopping criteria. After several numerical tests we used a grid with a meter of vertical resolution and 50 yr time-steps. In this simulation we assume perfectly sampled data, i.e. the age-depth distribution is available at the numerical grid points. The results are not reported here as the recovered accumulation and age-depth converges to the exact reference accumulation.

Then, we add a 1% random noise to the reference age-depth solution and apply our method to recover accumulation and age-depth. That is, we add to each sample of the reference age-depth value A_i an independent value sampled uniformly in the interval $[-0.01A_i, 0.01A_i]$. The results are in Figure 1. The recovered age-depth is nearly identical to the reference age-depth (under 0.1% difference), even in the deepest area of the record. On the other hand, the random noise introduce differences between recovered and reference accumulation: The difference increase with time from the present up to a value of about 10%.

Next, we investigate the effect of increasing noise. We compare the recovered accumulation from synthetic data obtained adding 1%, 5% and 10% random noise to the reference age-depth. The results are shown in Figure 2. The solution deteriorates when random noise increases, but the recovered accumulation only loses information for small wavelengths.

In the final numerical experiment (Fig. 3), we study the effect of not having data in an area. In the simulation we assumed that there is no data in $400\text{m} < z < 600\text{m}$ and that there is a 1% random noise in the synthetic age-depth. We find that the effect of not having any data over a given depth range of the bore hole on the inversion, is a period of time (area highlighted in Fig. 3) over which the retrieved accumulation is mainly constrained by the initially assumed profile and the regularization applied.

3.2 Recovering paleo-accumulation from James Ross Island ice core

In this Section, we apply the method to the ice core extracted from James Ross Island, a large island off the south-east side and near the north-eastern extremity of the Antarctic Peninsula. The data used in this section and its climatological implications are discussed in Mulvaney et al.
5 (2012) and Mulvaney et al. (2014).

Figure 4 shows the timeline for the James Ross Island ice core that is provided by fixed markers derived from local and global volcanic events with unequal estimated uncertainty (details in Mulvaney et al. (2012), Supplementary Table 1).

We assume that the shape function (Eq. 2) can be expressed as,

$$10 \quad \eta = \frac{\rho_I}{\rho} \eta_I \,,$$

where ρ is the measured density at a given depth, $\rho_I = 910 \text{ kg m}^{-3}$ is the reference density of ice, and η_I is the shape function for ice. We further assume that η_I follows a shallow ice approximation(e.g., Hutter, 1983),

$$\eta_I(s) = 1 - s \left(\frac{n+2}{n+1} - \frac{s^{n+1}}{n+1} \right) \,,$$

15 where s is the normalized depth ($s = (H - z)/H$). In order to measure the sensitivity to the uncertainty in ice-flow in the recovered age-depth distribution and accumulation record, we assume that the rheological index n varies in the range $2 \leq n \leq 5$.

We assume that there is no melting at the base of the dome as a temperature of -8.5C was recorded at the bottom of the ice-core. Also, because the time interval we are interested in is
20 only 3 kyr, we avoid the problem of guessing A_0 by expanding the simulation time until 10 kyr before present. That way, our solution is not sensitive to the value of A_0. Based on different numerical test we use a grid with 0.3 m resolution and 10 yr time-step.

The recovered age-depth (Fig. 4) follows the intervals of the observed measurements, and the uncertainty introduced by the ice-flow parameter n is smaller than a 1%, indiscernible in the

12

figure. On the other side, the recovered paleo-accumulation (Fig. 5) follows roughly the stable water isotope (δD), that is a proxy for temperature, but the result is not clear due to the small number of age markers (12 markers in 3 kyr) and the uncertainty introduced by the ice-flow parameter n. The uncertainty increases with time from the present and it becomes about 20%

5 of the estimated value after 3 kyr.

Finally, to estimate the sensitivity of the method to age-depth uncertainty, we use a basic Monte Carlo method (e.g., Campolongo et al., 2000). The error propagation is obtained by calculating the standard deviation, at a given depth, from a set of one hundred results for both accumulation and age-depth. For each one of the one hundred simulations, we resample the

10 measured age-depth observations assuming a normal distribution with standard deviation equal to one third of the uncertainty estimation (so that 99% of the samples lie within the range of observations).

The results are shown in Figure 6. The estimation of uncertainty in observed age-depth is variable from 1% at certain depths to about 10% in the deepest sections of the ice core. Similarly

15 to the uncertainty propagation introduced by the ice-flow (included in the Figure), uncertainty in accumulation increases with time from the present but reaching a maximum of about 15% after 3000 years.

4 Discussion

The quality of the information recovered from an inverse problem is always related to the quality

20 of the observed measurements and to the nature of the assumptions made in the forward model. In this paper, we have analysed the effect on paleo-accumulation (recovered information) of random noise, gaps and uncertainty in the age-depth distribution (observed measurements). We also evaluate the propagation of uncertainty introduced by assumptions in the forward model, that follows the compaction and compression of ice with time (Fig. 5). That uncertainty in

25 ice-flow is simplified in this study as the uncertainty in the rheological index n.

The experiments with synthetic data (Sec. 3.1) show that our method is robust: In perfectly sampled data (Fig. 2), it recovers the reference accumulation in the presence of random noise,

13

and, even when the increase in noise deteriorates the accumulation, it recovers time-averaged values as the details are first lost in the high temporal frequencies. Besides, when there are gaps in the data (Fig. 3), the retrieved profile is constrained by the regularization. We find that the smoothing in the accumulation transforms, after solving the forward model, into a smooth age-depth (Fig. 3). In contrast, a typical polynomial interpolation of the age-depth leads to spurious accumulation records due to the non-linearity introduced by the Age equation (Eq. 1) (Fudge et al., 2014).

The sensitivity analysis to the James Ross ice core data (Fig. 6), shows that between 1% and 10% of uncertainty in the observations results in similar uncertainty in paleo-accumulation. On the other hand, the propagation of uncertainty from the unknown parameter in ice flow model has a stronger effect on the accumulation (about 20%) than in the age-depth (under 1%).

It is not the objective of this study to evaluate the use of modelling in ice core dating, but this later result shows that, in our case study, there is a relatively small the sensitivity (under a 1%) of age-depth to uncertainty in ice-flow modelling. Age-depth depends on accumulation; and in the ice cores where accumulation can be extracted from temperature reconstructions and age-depth is constrained by fixed-markers, our test case supports the use of modelling in ice core dating (e.g., Parrenin et al., 2007a; Ruth et al., 2007; Lemieux-Dudon et al., 2010).

We only consider simplified ice flow shape functions (derived from Dansgaard and Johnsen (1969) in Sec. 3.1 and Shallow Ice Approximation in Sec. 3.2) as they are easier to analyze and because our aim is to incorporate measured full-depth vertical velocity as they become available in the future. Our main assumption is that the spatial variability of the velocity depends on compaction and rheology, and the time dependence is proportional to the combined result of accumulation and surface thinning. This assumption is partially supported by the perturbation analysis of Wilchinsky and Chugunov (1997), that assumes isothermal ice; but we do not consider the effect of time evolution on firnification (e.g., Arthern and Wingham, 1998), temperature along the core (e.g., Nereson and Waddington, 2002), ice fabric (e.g., Martín and Gudmundsson, 2012), dome migration (e.g., Martín et al., 2009), horizontal advection or thinning (e.g., Huybrechts et al., 2007).

14

More complete ice-flow models can be incorporated into the inverse problem. The method consist of adding the weak form of the system of equations for the velocity (ice-flow model) to the Lagrangian $\mathcal{L}$ in Equation 5 (e.g., Petra and Stadler, 2011, Sec. 3). The challenge is that the data extracted from the ice-core, that is constraining the climatic reconstruction, is one-dimensional but the ice-flow problem is three-dimensional with a poorly constrained rheology. The main issue, when considering horizontal advection, is that the ice along the core could have been deposited at the surface at a different position that the actual ice-core surface position, and ice-domes near the coast are areas where the gradients in surface accumulation can be high (Lenaerts et al., 2014). We expect that the analysis of full-depth velocity datasets near ice-rises (Kingslake et al., 2014) provides information on spatial variations of ice-flow on ice-domes and help to reconstruct the paleo-accumulation records.

5 Conclusions

The present study describes a novel application of an adjoint-based method to derive paleo-accumulation records from ice core chronology. The method is designed for ice cores in coastal areas of Antarctica and Greenland because it does not rely on temperature reconstructions.

Our approach is to follow a Lagrange method for constrained optimization, commonly employed in CFD inverse problems governed by partial differential equations. We apply our method to synthetic and existing data from the James Ross Island ice core. We show that the method is robust, as it retrieves paleo-accumulation from data with random noise and it reacts well to gaps in the data. We also show that the quality of the paleo-accumulation depends on the quality of the age-depth observations, uncertainty and sampling, and the uncertainty in ice-flow.

Besides, in our case study on James Ross Island ice core, where full-depth velocity measurements are not available, the largest uncertainty in the inferred paleo-accumulation is a consequence of the unknown ice-flow parameters. It increases with time until a maximum of about 20%. In addition, an uncertainty in the chronology between 1% and 10% propagates into a similar uncertainty in paleo-accumulation.

Our ambition is to incorporate to the method full-depth vertical velocity obtained with phase sensitive radar, in order to reduce the uncertainty introduced by ice-flow modelling, and a detailed chronology, provided by ice core analysis, in order to obtain a optimized chronology and a detailed paleo-accumulation record.

Appendix A: Derivation of the model system of equations

The Lagrangian $\mathcal{L}$ (Eq. 5) has been defined so that its minimization is equivalent to the minimization of J (Eq. 3) , the difference between observations and model results, and the forward model (Eq. 1). In this Section, we calculate the functional derivative of $\mathcal{L}$ with respect to the Lagrangian multiplier λ, to check that the minimization of $\mathcal{L}$ is constrained to verify the forward model (Eq. 1); with respect to the age, to obtain the adjoint problem (Eq. 6); and with respect to the control variable a, to calculate its gradient g_a (Eq. 7). The gradients for melting (g_m) and initial age distribution (g_A) in Equation 7 can be obtained in a similar way.

By definition, the functional derivative of $\mathcal{L}$ with respect to the Lagrange multiplier λ in a direction $\bar{\lambda}$ is,

$$\delta_\lambda \mathcal{L}(a, m, A_0; A, \lambda)(\bar{\lambda}) = \left[\frac{d}{d\epsilon} \mathcal{L}(a, m, A_0; A, \lambda + \epsilon \bar{\lambda}) \right]_{\epsilon=0},$$

where ϵ is a constant and $\bar{\lambda}$ is an arbitrary function.

The result of setting to zero the functional derivative of $\mathcal{L}$ with respect to the Lagrange multiplier is,

$$\delta_\lambda \mathcal{L}(a, m, A_0; A, \lambda)(\bar{\lambda}) = \int\limits_0^T \int\limits_0^H \bar{\lambda}(\partial_t A + w \, \partial_z A - 1) \, dz \, dt + \int\limits_0^H \bar{\lambda}(z, 0) \, [A(z, 0) - A_0] \, dz = 0,$$

which is the weak form of the forward model (Eq. 1). That is, because $\bar{\lambda}$ is an arbitrary function, the Equation is true when the age distribution verifies the forward model.

16

Similarly, by setting to zero the functional derivative of $\mathcal{L}$ with respect to the Age, we obtain:

$$\delta_A \mathcal{L}(a, m, A_0; A, \lambda)(\bar{A}) = \int\limits_0^H \bar{A} \frac{[A(z,T) - A_d]}{\sigma_d} P_d \, dz$$

$$+ \int\limits_0^T \int\limits_0^H \lambda(\partial_t \bar{A} + w \, \partial_z \bar{A}) \, dz \, dt + \int\limits_0^H \lambda(z,0) \bar{A}(z,0) \, dz = 0.$$

We then integrate by parts $\lambda \partial_t \bar{A}$ with respect to time and $\lambda w \, \partial_z \bar{A}$ with respect to z,

$$\int\limits_0^H \bar{A} \frac{[A(z,T) - A_d]}{\sigma_d} P_d \, dz - \int\limits_0^T \int\limits_0^H \bar{A} \left[\partial_t \lambda + \partial_z(w\lambda) \right] dz \, dt$$

$$+ \int\limits_0^H \left[\lambda(z,T) \bar{A}(z,T) - \lambda(z,0) \bar{A}(z,0) \right] dz$$

$$+ \int\limits_0^T \left[\lambda(H,t) w(H) \bar{A}(H,t) - \lambda(0,t) w(0) \bar{A}(0,t) \right] dt$$

$$+ \int\limits_0^H \lambda(z,0) \bar{A}(z,0) \, dz = 0.$$

After setting $\bar{A}(H,t)$ to zero, as it has to have the same properties that the age-depth distribution that is null at the surface, we obtain,

$$\int\limits_0^H \bar{A} \left[\lambda + \frac{[A(z,T) - A_d]}{\sigma_d} P_d \right] dz - \int\limits_0^T \int\limits_0^H \bar{A} \left[\partial_t \lambda + \partial_z(w\lambda) \right] dz \, dt - \int\limits_0^T \bar{A}(0,t) \lambda(0,t) w(0) dt = 0,$$

that is the weak form of the Adjoint problem (Eq. 6).

17

Finally, we calculate the gradient of $\mathcal{L}$ with respect to the accumulation as,

$$\delta_a \mathcal{L}(a, m, A_0; A, \lambda)(\bar{a}) = \gamma_a^R \int\limits_0^T \left[\partial_t a \partial_t \bar{a} \right] dt + \int\limits_0^T \int\limits_0^H \lambda \bar{a} \eta \partial_z A \, dz \, dt \; ,$$

that, applying integration by parts to the first term of the right-hand side, can be written as,

$$\delta_a \mathcal{L}(a, m, A_0; A, \lambda)(\bar{a}) = \gamma_a^R \int\limits_0^T \bar{a} \left[-\partial_t^2 a \int\limits_0^H \lambda \bar{a} \eta \partial_z A \, dz \right] dt + \bar{a}(T) \partial_t a(T) - \bar{a}(0) \partial_t a(0) = 0,$$

that is the weak form of the gradient defined in Equation 7.

References

Armijo, L.: Minimization of functions having Lipschitz continuous first partial derivatives., Pacific Journal of Mathematics, 16, 1–3, http://projecteuclid.org/euclid.pjm/1102995080, 1966.

Arthern, R. and Wingham, D.: The Natural Fluctuations of Firn Densification and Their Effect on the Geodetic Determination of Ice Sheet Mass Balance, Climatic Change, 40, 605–624, doi:10.1023/A:1005320713306, http://dx.doi.org/10.1023/A%3A1005320713306, 1998.

Bromwich, D. and Robasky, F.: Recent precipitation trends over the polar ice sheets, Meteorology and Atmospheric Physics, 51, 259–274, doi:10.1007/BF01030498, http://dx.doi.org/10.1007/BF01030498, 1993.

Campolongo, F., Saltelli, A., Sorensen, T., and Tarantola, S.: Hitchhiker's guide to sensitivity analysis, in: Sensitivity Analysis, edited by Saltelli, A., Chan, K., and Scott, M., pp. 15–47, Wiley, Chichester, UK, 2000.

Corr, H. F. J., Jenkins, A., Nicholls, K. W., and Doake, C. S. M.: Precise measurement of changes in ice-shelf thickness by phase-sensitive radar to determine basal melt rates, Geophysical Research Letters, 29, 73–1–74–4, doi:10.1029/2001GL014618, http://dx.doi.org/10.1029/2001GL014618, 2002.

Dansgaard, W. and Johnsen, S. J.: A flow model and a time scale for the ice core from Camp Century, Greenland, J. Glaciol., 8, 215–223, 1969.

Dennis, Jr., J. E. and Schnabel, R. B.: Numerical Methods for Unconstrained Optimization and Nonlinear Equations (Classics in Applied Mathematics, 16), Soc for Industrial & Applied Math, 1996.

EPICA community members: Eight glacial cycles from an Antarctic ice core, Nature, 429, 623–628, doi:10.1038/nature02599, http://dx.doi.org/10.1038/nature02599, 2004.

Fudge, T. J., Waddington, E. D., Conway, H., Lundin, J. M. D., and Taylor, K.: Interpolation methods for Antarctic ice-core timescales: application to Byrd, Siple Dome and Law Dome ice cores, Climate of the Past Discussions, 10, 65–104, doi:10.5194/cpd-10-65-2014, http://www.clim-past-discuss.net/10/65/2014/, 2014.

Hammer, C., Clausen, H., Dansgaard, W., Gundestrup, N., Johnsen, S., and Reeh, N.: Dating of Greenland ice cores by flow models, isotopes, volcanic debris, and continental dust, Journal of Glaciology, 20, 3–26, 1978.

Hansen, P. C.: The L-Curve and its Use in the Numerical Treatment of Inverse Problems, in: in Computational Inverse Problems in Electrocardiology, ed. P. Johnston, Advances in Computational Bioengineering, vol. 4, pp. 119–142, http://citeseerx.ist.psu.edu/viewdoc/summary?doi=10.1.1.33.6040, 2000.

Hindmarsh, R. C. A.: Notes on basic glaciological computational methods and algorithms, in: Continuum Mechanics and Applications in Geophysics and the Environment, edited by Greve, R., Ehrentraut, H., Wang, Y., and Straughan, B., pp. 47–60, Springer-Verlag, Berlin, 2001.

Hutter, K.: Theoretical Glaciology, Reidel, Dordrecht, 1983.

Huybrechts, P., Rybak, O., Pattyn, F., Ruth, U., and Steinhage, D.: Ice thinning, upstream advection, and non-climatic biases for the upper 89% of the EDML ice core from a nested model of the Antarctic ice sheet, Climate of the Past, 3, 577–589, doi:10.5194/cp-3-577-2007, http://www.clim-past.net/3/577/2007/, 2007.

Jenkins, A., Corr, H. F., Nicholls, K. W., Stewart, C. L., and Doake, C. S.: Interactions between ice and ocean observed with phase-sensitive radar near an Antarctic ice-shelf grounding line, Journal of Glaciology, 52, 325–346, doi:doi:10.3189/172756506781828502, http://www.ingentaconnect.com/content/igsoc/jog/2006/00000052/00000178/art00001, 2006.

Kapsner, W. R., Alley, R. B., Shuman, C. A., Anandakrishnan, S., and Grootes, P. M.: Dominant influence of atmospheric circulation on snow accumulation in Greenland over the past 18,000 years, Nature, 373, 52–54, doi:10.1038/373052a0, http://dx.doi.org/10.1038/373052a0, 1995.

Kingslake, J., Hindmarsh, R. C. A., Aðalgeirsdóttir, G., Conway, H., Corr, H. F. J., Gillet-Chaulet, F., Martín, C., King, E. C., Mulvaney, R., and Pritchard, H. D.: Full-depth englacial vertical ice sheet velocities measured using phase-sensitive radar, Journal of Geophysical Research: Earth Surface, pp. n/a–n/a, doi:10.1002/2014JF003275, http://dx.doi.org/10.1002/2014JF003275, 2014.

Lemieux-Dudon, B., Blayo, E., Petit, J.-R., Waelbroeck, C., Svensson, A., Ritz, C., Barnola, J.-M., Narcisi, B. M., and Parrenin, F.: Consistent dating for Antarctic and Greenland ice cores, Quaternary Science Reviews, 29, 8 – 20, doi:http://dx.doi.org/10.1016/j.quascirev.2009.11.010, http://www.sciencedirect.com/science/article/pii/S0277379109003734, 2010.

Lenaerts, J. T. M., Brown, J., van den Broeke, M. R., Matsuoka, K., Drews, R., Callens, D., Philippe, M., Gorodetskaya, I. V., van Meijgaard, E., Reijmer, C. H., Pattyn, F., and van Lipzig, N. P. M.: High variability of climate and surface mass balance induced by Antarctic ice rises, Journal of Glaciology, 60, doi:10.3189/2014JoG14J040, 2014.

Martín, C. and Gudmundsson, G. H.: Effects of nonlinear rheology, temperature and anisotropy on the relationship between age and depth at ice divides, The Cryosphere Discuss., 6, 2221–2245, doi:10.5194/tcd-6-2221-2012, 2012.

Martín, C., Hindmarsh, R. C. A., and Navarro, F. J.: On the effects of divide migration, along-ridge flow, and basal sliding on isochrones near an ice divide, Journal of Geophysical Research: Earth Surface, 114, F02 006, doi:10.1029/2008JF001025, http://dx.doi.org/10.1029/2008JF001025, 2009.

Mulvaney, R., Abram, N. J., Hindmarsh, R. C. A., Arrowsmith, C., Fleet, L., Triest, J., Sime, L. C., Alemany, O., and Foord, S.: Recent Antarctic Peninsula warming relative to Holocene climate and ice-shelf history, Nature, 489, 141–144, doi:10.1038/nature11391, http://dx.doi.org/10.1038/nature11391, 2012.

Mulvaney, R., Triest, J., and Alemany, O.: The James Ross Island and the Fletcher Promontory ice-core drilling projects, Annals of Glaciology, 68, accepted, 2014.

Nereson, N. A. and Waddington, E. D.: Isochrones and isotherms beneath migrating ice divides, J. Glaciol., 48 (160), 95–108, 2002.

Parrenin, F., Jouzel, J., Waelbroeck, C., Ritz, C., and Barnola, J.-M.: Dating the Vostok ice core by an inverse method, Journal of Geophysical Research: Atmospheres, 106, 31 837–31 851, doi:10.1029/2001JD900245, http://dx.doi.org/10.1029/2001JD900245, 2001.

Parrenin, F., Barnola, J.-M., Beer, J., Blunier, T., Castellano, E., Chappellaz, J., Dreyfus, G., Fischer, H., Fujita, S., Jouzel, J., Kawamura, K., Lemieux-Dudon, B., Loulergue, L., Masson-Delmotte, V., Narcisi, B., Petit, J.-R., Raisbeck, G., Raynaud, D., Ruth, U., Schwander, J., Severi, M., Spahni, R., Steffensen, J. P., Svensson, A., Udisti, R., Waelbroeck, C., and Wolff, E.: The EDC3 chronol-

ogy for the EPICA Dome C ice core, Climate of the Past, 3, 485–497, doi:10.5194/cp-3-485-2007, http://www.clim-past.net/3/485/2007/, 2007a.

Parrenin, F., Dreyfus, G., Durand, G., Fujita, S., Gagliardini, O., Gillet, F., Jouzel, J., Kawamura, K., Lhomme, N., Masson-Delmotte, V., Ritz, C., Schwander, J., Shoji, H., Uemura, R., Watanabe, O., and
5 Yoshida, N.: 1-D-ice flow modelling at EPICA Dome C and Dome Fuji, East Antarctica, Clim. Past., 3, 243–259, doi:10.5194/cp-3-243-2007, http://www.clim-past.net/3/243/2007/, 2007b.

Petra, N. and Stadler, G.: Model variational inverse problems governed by partial differential equations, ICES Report 11-05, The Institute for Computational Engineering and Sciences, The University of Texas at Austin, 2011.

10 Rasmussen, S. O., Andersen, K. K., Svensson, A. M., Steffensen, J. P., Vinther, B. M., Clausen, H. B., Siggaard-Andersen, M.-L., Johnsen, S. J., Larsen, L. B., Dahl-Jensen, D., Bigler, M., Röthlisberger, R., Fischer, H., Goto-Azuma, K., Hansson, M. E., and Ruth, U.: A new Greenland ice core chronology for the last glacial termination, Journal of Geophysical Research: Atmospheres, 111, D06 102, doi:10.1029/2005JD006079, http://dx.doi.org/10.1029/2005JD006079, 2006.

15 Ruth, U., Barnola, J.-M., Beer, J., Bigler, M., Blunier, T., Castellano, E., Fischer, H., Fundel, F., Huybrechts, P., Kaufmann, P., Kipfstuhl, S., Lambrecht, A., Morganti, A., Oerter, H., Parrenin, F., Rybak, O., Severi, M., Udisti, R., Wilhelms, F., and Wolff, E.: "EDML1": a chronology for the EPICA deep ice core from Dronning Maud Land, Antarctica, over the last 150 000 years, Climate of the Past, 3, 475–484, doi:10.5194/cp-3-475-2007, http://www.clim-past.net/3/475/2007/, 2007.

20 Spiegelman, M. and Katz, R. F.: A semi-Lagrangian Crank-Nicolson algorithm for the numerical solution of advection-diffusion problems, Geochemistry, Geophysics, Geosystems, 7, Q04 014, doi:10.1029/2005GC001073, http://dx.doi.org/10.1029/2005GC001073, 2006.

Staniforth, A. and Côté, J.: Semi-Lagrangian Integration Schemes for Atmospheric Models- A Review., Monthly Weather Review, 119, 2206–2223, 1991.

25 Tröltzsch, F.: Optimal Control of Partial Differential Equations: Theory, Methods, and Applications, Graduate Studies in Mathematics, American Mathematical Society, http://books.google.co.uk/books?id=MmkqgJKrnDwC, 2010.

van Ommen, T. D. and Morgan, V.: Snowfall increase in coastal East Antarctica linked with southwest Western Australian drought, Nature Geosci, 3, 267–272, doi:10.1038/ngeo761,
30 http://dx.doi.org/10.1038/ngeo761, 2010.

Watanabe, O., Jouzel, J., Johnsen, S., Parrenin, F., Shoji, H., and Yoshida, N.: Homogeneous climate variability across East Antarctica over the past three glacial cycles, Nature, 422, 509–512, doi:10.1038/nature01525, http://dx.doi.org/10.1038/nature01525, 2003.

Wilchinsky, A. V. and Chugunov, V. A.: Modelling ice-divide dynamics by perturbation methods, J. Glaciol., 43, 352–358, 1997.
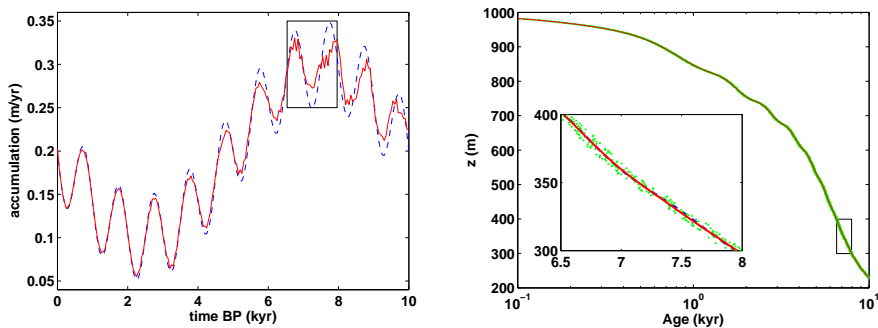
Figure 1. Recovered accumulation (red, left panel) and age-depth distribution (red, right panel) from age-depth synthetic data (green, right panel). The synthetic age-depth distribution has been obtained by adding 1% uniform noise to the reference solution (blue right-panel) derived from the reference accumulation record (blue, left panel). Inset in the right panel zooms into the age-depth profile in an area that is highlighted both in the accumulation record and in the age-depth distribution.
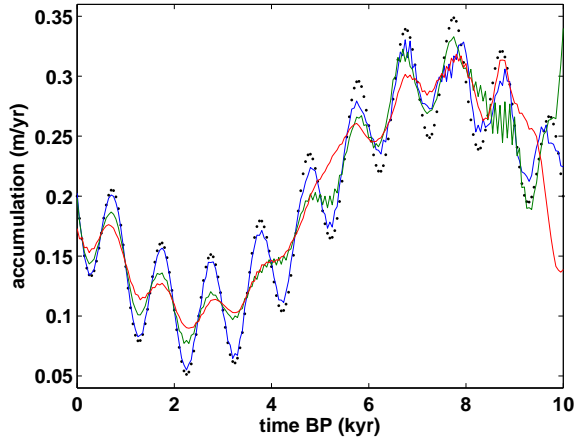
Figure 2. Recovered Accumulation from the synthetic age-depth distribution obtained adding 1% (blue), 5% (green) and 10% (red) uniform noise to the solution derived from the reference accumulation (dotted line).
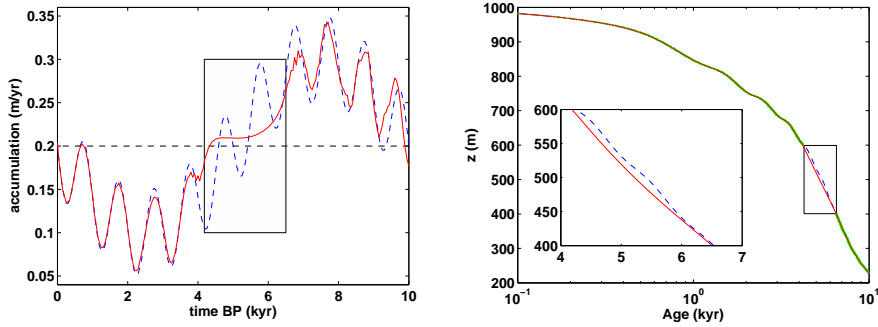
Figure 3. Recovered accumulation (red, left panel) and age-depth distribution (red, right panel) from age-depth synthetic data (green, right panel). The synthetic age-depth distribution has been obtained by adding 1% uniform noise to the reference solution (blue right-panel) derived from the reference accumulation record (blue, left panel), and considering a gap in the data ($400\,\mathrm{m} < z < 600\,\mathrm{m}$). Inset in the right panel zooms into the age-depth results where there is a gap in the age-depth data.
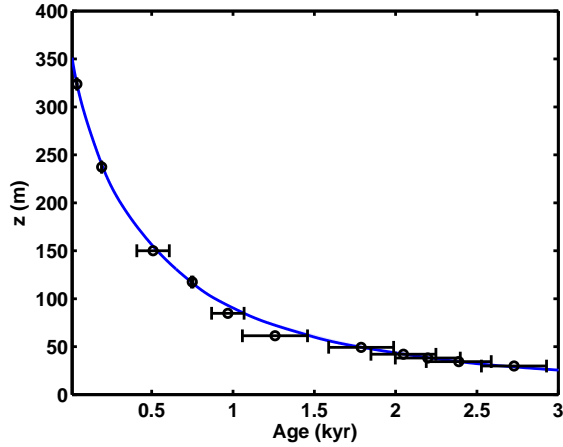
Figure 4. Recovered age-depth (blue) and observed age-depth (black) from (Mulvaney et al., 2012). The uncertainty in recovered accumulation due to unknown ice-flow parameter n ($2 \leq n \leq 5$) is indiscernible in the plot.
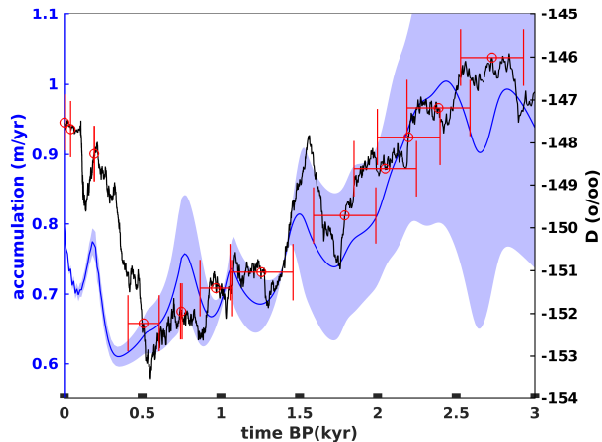
Figure 5. Recovered accumulation (blue) from James Ross ice core observed age-depth and stable water isotope δD (black). Red symbols represent the uncertainty in age-depth at the points where absolute markers where found (Mulvaney et al., 2012). The area in blue represents uncertainty in recovered accumulation due to unknown ice-flow parameter n ($2 \leq n \leq 5$). The stable water isotope δD has not been used for the inversion and is plotted only for reference.
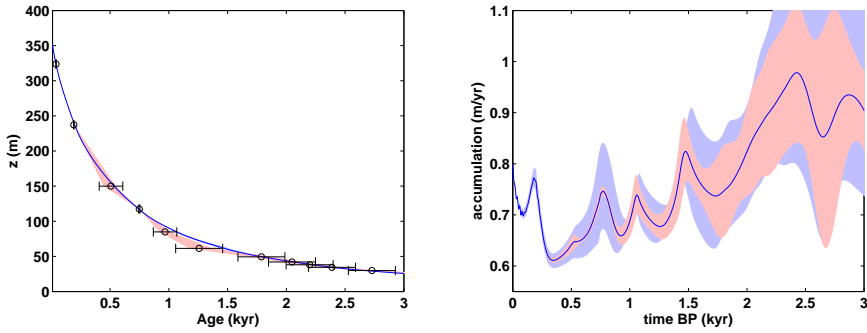
Figure 6. Sensitivity analysis to uncertainty in chronology (red) and shape function η (blue). The uncertainty in chronology is assumed to follow a normal distribution. The uncertainty in the shape function η is represented by the range $2 \leq n \leq 5$ for the rheological index in the Glen flow law.

28